

## Specific-heat jump of superconducting lamellas with pair-breaking boundary conditions

P. Manuel

*Laboratoire de Physique des Solides,\* Université Paris-Sud, 91405, Orsay, France*

J. J. Veysié

*Conservatoire National des Arts et Métiers, 292 rue Saint-Martin, 75003 Paris*

(Received 2 December 1974; revised manuscript received 8 December 1975)

Specific-heat measurements are reported for aluminum foils and tin films near their superconductive transition point. Surface pair-breaking effects were induced by three different means: the implantation of gadolinium impurities, the superimposition of the stray fields from iron deposits, and the proximity effect with chromium. The specific-heat jump reduction and the shift in the critical temperature are analyzed within the framework of Fulde and Moormann calculations on the thermodynamical properties of superconducting contacts. On the whole a fair agreement between experiment and theory is observed, but some limitations of the theoretical treatment and some difficulties in the experimental situation are discussed.

### I. INTRODUCTION

It is well known that the temperature-dependent coherence length, which gives the scale of variation of the pair potential  $\Delta(x)$  in a superconductor, diverges at  $T_{c0}$ , the transition temperature in zero field. Any particular boundary condition, such as one prescribed by proximity effects, induces a change in the spatial variation of  $\Delta$ , which is consequently of comparatively long range around  $T_{c0}$ . Then a modification in the bulk thermodynamical properties of the superconductor is expected near the transition point, even for specimen thicknesses very much greater than the zero-temperature value  $\xi_0$  of the coherence length.

The problem has been theoretically investigated by Fulde and Moorman (FM).<sup>1</sup> For a rather thick superconducting film, limited by the planes  $x=0$  and  $x=d_s$  and subjected to the boundary conditions  $[\Delta(x)]_{x=0} = 0$  (strong pair-breaking effect) and  $[d\Delta(x)/dx]_{x=d_s} = 0$  (free surface), the main predictions of FM theory are the following.

(a) The specific-heat jump  $\Delta\bar{C}$  at  $T_c$  is reduced by a factor  $\frac{2}{3}$  as compared with the jump  $\Delta\bar{C}_0$  observed at  $T_{c0}$  with an unperturbed sample.

(b) The transition point  $T_c$  is shifted below the unperturbed value  $T_{c0}$  according to the formula:

$$\ln(t_c) = -[\pi\Lambda(t_c)/2d_s]^2 \quad \text{with } t_c = T_c/T_{c0}$$

and

$$\Lambda^2(t_c) \approx \frac{0.88}{3} \xi_0 l \left\{ \left( \frac{\pi}{2} \right)^2 + \frac{l}{0.88\xi_0} \right. \\ \left. \times \left[ \psi\left(\frac{1}{2}\right) - \psi\left(\frac{1}{2} + \frac{0.88}{2} \frac{\xi_0}{l}\right) \right] \right\},$$

where  $l$  is the electron mean free path and  $\psi(x)$  is the di- $\gamma$  function. The jump in the specific heat at  $T_c$  is thus a much more sensitive measure of the

pair-breaking boundary condition than the associated shift of  $T_c$ .

(c) Below  $T_c$  the specific-heat jump is followed by a further increase of the difference  $\Delta\bar{C}(T)$  between the specific heats of the superconducting and normal states;  $\Delta\bar{C}(T)$  tends more and more rapidly towards the behavior representative of an unperturbed sample as the slabs grow thicker and thicker. There are numerical computations by FM which give the thermal dependence of the reduced specific-heat difference  $\Delta C(t) = \Delta\bar{C}(t)/\Delta\bar{C}_0$  vs  $t = T/T_{c0}$  for different values of  $d_s/\Lambda(t_c)$  or  $t_c$ . However, it must be remembered that these results have been derived under the usual assumptions of the generalized Ginzburg-Landau equations, with an expansion in terms of the order parameter up to the fourth order only. Such an approximation is known to yield the correct value of the specific-heat jump right at  $T_c$ , but higher-order terms must be taken into account if the specific heat is to be obtained in any finite temperature interval.<sup>2</sup> Thus, below  $T_c$ , only a qualitative agreement can be expected between experiment and FM theory.

Nevertheless, FM computations lead to valuable predictions concerning the magnitude of  $d_s$  which are of practical interest. The validity of FM theory is subjected to the condition  $1 - t_c \ll 1$  which approximately requires  $d_s/\Lambda(t_c) > 10$ . On the other hand, with very thick films the specific-heat curve below  $T_c$  will be too close to the bulk curve for any deviation to be accurately resolved by experiment: for a fair observation of the effect one would need approximately  $d_s/\Lambda(t_c) < 70$ . Thus the suitable thickness for experimental investigation appears to be rather critical.

Attempts to measure the modifications of the specific-heat jump induced by the proximity effect have been previously carried out on lamellar Pb-Sn

eutectic alloys.<sup>3</sup> Such systems do not permit a sensitive check of theory, first because the widths of the lamellas and the electron mean free paths within them cannot be accurately determined, second because the substantial broadening of the transition breadths which results from the strains, the inhomogeneous impurity concentrations, and the variations of layer thicknesses, makes the definition of the specific-heat jump rather uncertain.

The present work is an attempt to obtain more tractable experimental data by using samples which were, as far as possible, geometrically and physically better defined. The investigations have been carried out on single superconducting layers. Quite apart from the problems concerning the measurements of the exceedingly small heat capacities involved, some experimental complications still remain: the influence of stresses on the superconductive parameters, and the achievement of some well-defined pair-breaking boundary condition.

Since it has been previously demonstrated that the ac calorimetry technique is capable of yielding accurate measurements on thin films,<sup>4</sup> only the basic features of the experimental setup will be reported in Sec. II. In Sec. III a set of experiments on aluminum slabs will be presented and discussed: the characteristics of the samples used excluded the possibility that pair-breaking effects could be conveniently achieved by the proximity effect, and more complicated methods have been worked out, such as the implantation of gadolinium impurities and the application of stray fields from deposits of iron. On the other hand, the pair-breaking effect resulting from the proximity effect of chromium has been investigated in the case of tin films and Sec. IV will be devoted to the description and discussion of the results. Section V will be devoted to the conclusions which can be drawn concerning the limitations of the present investigation and of FM theory.

## II. CALORIMETRY

The basic features of the steady-state ac calorimetry method are now sufficiently well known for any additional report to be unnecessary.<sup>5</sup> Our experimental setup was designed a few years ago in order to measure heat capacities from 0.3 up to about 10 K with an absolute accuracy better than 2%. The cryostat and the electronic instrumentation have been described previously.<sup>6</sup> However, for the present work a new lock-in amplifier with an improved noise figure was used, yielding heat-capacity measurements with a scatter less than a few  $10^{-4}$ . The data were directly processed by a desk computer interconnected with a digital plotter.

The sample holder consisted of a thin slab of

sapphire (0.3 mm thick) on one side of which the samples were glued or evaporated. A silver heater was evaporated on the opposite side and a temperature sensor was glued on. The sapphire substrate was fastened to the heat sink by four thin silvered Mylar strips, with the thickness of the silver chosen so as to give a sample-to-bath thermal relaxation time of approximately 1 sec. These strips ensured simultaneously the electrical connections of the heater and of the temperature sensor. Extra evaporation of silver spots was made to provide the necessary electrical contacts. The whole assembly was surrounded by a copper shield fastened to the heat sink. Its reduced temperature was controlled within  $10^{-5}$ . The earth's magnetic field was shielded to a residual value of less than  $5 \times 10^{-2}$  Oe by a  $\mu$  metal sheet at room temperature and a superconducting lead cylinder in the helium bath. Magnetic fields, up to 70 kOe if necessary, could be supplied by a superconducting coil.

The temperature sensors were carbon lamellas obtained by grinding down Allen Bradeley resistors to a thickness of approximately 20  $\mu$ m. For the measurements on aluminum the temperature range of interest was 0.8–1.4 K and 10- $\Omega$ ,  $\frac{1}{4}$ -W resistors were used. In the case of tin the temperature range was 2.5–4 K and 33  $\Omega$ ,  $\frac{1}{4}$ -W resistors were used. The measuring power level in the sensors was kept sufficiently low so that temperature gradients could be safely ignored. It was kept between  $10^{-10}$  and  $5 \times 10^{-10}$  W in the range 0.8–1.4 K, and between  $5 \times 10^{-10}$  and  $1.5 \times 10^{-9}$  W in the range 2.5–4 K. For each run the sensors were calibrated against a reference germanium thermometer on the heat sink. Typically 15 calibration points were taken in the temperature range of interest. The resistance temperature characteristics were fitted to a smooth curve of the form

$$\frac{1}{T} = \sum_{n=1}^3 A_n (\ln R)^n$$

by a least-square routine. The errors of this fitting function from the calibration data were less than  $10^{-3}$  in reduced temperature. We used three different standards for the calibration of the reference germanium thermometer<sup>7</sup>: the vapor pressure of  $^3\text{He}$ , the paramagnetic susceptibility of cerium magnesium nitrate, and a calibrated germanium thermometer<sup>8</sup> for the high-temperature side of the measurements.

The experimental accuracy in the heat-capacity measurements by the ac method rests on the requirement that the sample assembly be in thermal equilibrium on a time scale much shorter than the period of the temperature oscillations. Following Sullivan and Seidel,<sup>5</sup> a procedure has been commonly used by several workers in which two kinds

of limiting factors are considered separately. On one hand, the finite thermal conductivity of the sample is taken into account by means of an internal relaxation time which is calculated under the assumption of a one-dimensional heat flow. The diffusion effect in the conductance linking the sample to the heat sink can be considered similarly.<sup>9</sup> On the other hand, the finite conductances interconnecting the various components of the sample assembly are taken into account while the internal thermal conductivities of these components are assumed to be infinite. This procedure results in a set of time constants. All of them were kept shorter than a few times  $10^{-4}$  sec in our system. But, in view of the approximations involved in such a model, we performed a complete numerical treatment of the heat diffusion problem in our sample assembly. A detailed description of this work has been given elsewhere.<sup>10</sup> The result is that, in the worst case, the relative inaccuracy introduced by the thermal diffusion effect is less than  $10^{-3}$  when the frequency of the ac temperature modulation is 24 Hz.

### III. EXPERIMENTS ON ALUMINUM

Aluminum presents three main advantages for an experimental investigation of the effect of a pair-breaking boundary condition on the specific-heat jump. First, the transition width of pure samples is quite narrow (typically  $\sim 10^{-3}$  K) so that a fairly good definition of the specific-heat

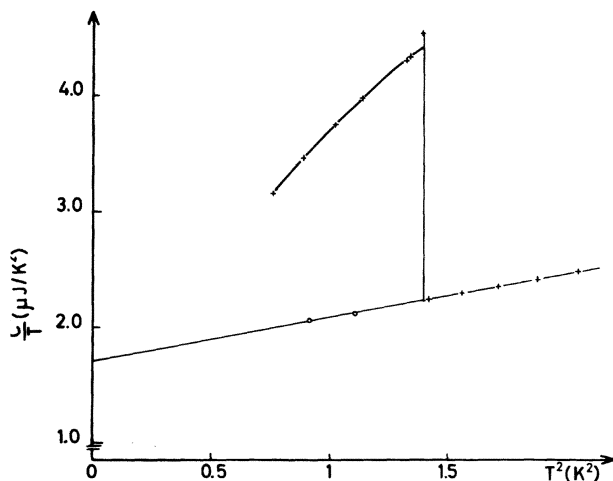


FIG. 1. Raw data for the heat capacity of sample Al (1) (pure aluminum foil) with sample holder. Crosses (+) are experimental points in the superconducting state, circles (o) are normal-state data. Points in the transition have not been reproduced, with the exception of one point at the very peak which has been left to indicate the order of magnitude of the effect of the residual magnetic field.

jump can be achieved. Second, the critical temperature is rather low so that the jump contributes for quite an appreciable change in the total heat capacity (typically 50% in the present experiments). Third, the coherence length is comparatively large (with a zero-temperature value  $\xi_0 = 1.6 \mu\text{m}$ ), and it follows from the foregoing discussion of FM theory that the thicknesses of practical interest are of the order of a few times  $10 \mu\text{m}$ , so that the heat capacities involved are not vanishingly small. However, if a sample with such a thickness was to be obtained by the usual vacuum evaporation techniques, the adherence of the metal to the substrate would be very poor and would result, sooner or later, in peeling of the film. Consequently we used a laminated foil of aluminum which was glued on the sapphire substrate with an epoxy cement heat-cured at a temperature of the order of  $130^\circ\text{C}$ . The foil was  $25 \mu\text{m}$  thick and had a stated purity of 99.995% and a measured resistivity ratio of  $100 \pm 1$ . From these data we deduced  $l \approx 4 \mu\text{m}$ ,  $\Lambda(t_c) = 1.04 \mu\text{m}$ , and  $d_s/\Lambda(t_c) = 24$ .

#### A. Unperturbed sample [Al(1)]

A first set of data was taken on a slab weighing  $31.5 \times 10^{-3}$  g which had been cut out of the raw aluminum foil without any surface treatment. Hereafter these data will be referred to as the unperturbed state data, or Al(1) data. The total heat capacity of the assembly  $C^*$ , including Al(1) and the sample holder, was successively measured in a nearly zero field and in a field of about 300 Oe. The results appear in Fig. 1. The quantities of interest for the present investigation, i.e., the zero-field transition point  $T_{c_0}$  and the specific-heat jump  $\Delta\bar{C}_0$ , were both directly obtained from these raw data as will be explained later. But, for a further comparison of our experiments with existing data, we measured the heat capacity of the sample holder in a separate run, and thus we deduced for Al(1) the normal-state electronic specific-heat coefficient  $\gamma = 1.42 \text{ mJ/mole K}^2$  and the ratio  $[(\bar{C}_{es} - \gamma T)/\gamma T]_{T_c} = 1.32$ .  $T_{c_0}$  and  $\Delta\bar{C}_0$  were determined in the following way.

Upon heating through the critical region, the specific heat was observed to go through a narrow peak and then to abruptly recover the normal-state value. Such a behavior—which was observed on the other aluminum specimens as well—can be easily understood as being due to the incomplete shielding of the surrounding magnetic field which induces a first-order transition. Since the peak was sharp and quite reproducible, the temperature at which it occurred was taken as  $T_{c_0}$ , yielding the value  $T_{c_0} = 1.183 \pm 0.001 \text{ K}$ . On the other hand, the

experimental data points represent an averaged value of the heat capacity over the narrow temperature range  $\delta T \approx 6 \times 10^{-3}$  K which was covered by the induced thermal oscillations. It may then be inferred that the measurements performed in the interval  $(T_{c_0} - \delta T, T_{c_0} + \delta T)$  are not really significant for determining the specific-heat jump. Therefore  $\Delta\bar{C}_0$  was calculated by fitting the data points obtained outside the critical interval to a power-series expansion in terms of the temperature and by extrapolation to  $T = T_{c_0}$ . This procedure gives  $\Delta\bar{C}_0 = 2.21 \pm 0.02$  mJ/mole K.

All these results are in quite satisfactory agreement with previous results on bulk aluminum samples.<sup>11</sup> Furthermore, our measurements yield a straightforward determination of the difference  $\Delta\bar{C}(T) = \bar{C}_s(T) - \bar{C}_n(T)$  between the superconducting and normal-state specific heats of Al(1), and the observed value for the slope of the reduced specific-heat difference  $[d\Delta C(t)/dt]_{t=1} = 2.5 \pm 0.2$  is in fair agreement with the theoretical value 2.63 of Ref. 2. However, it is worth noting that the latter is at variance with the FM prediction:  $[d\Delta C(t)/dt]_{t=1} = 4$  (Fig. 2). As pointed out in the foregoing discussion the discrepancy results from the approximation made in FM theory where the free energy was expanded in terms of the order parameter up to the fourth order only.

#### B. Gadolinium-implanted sample [Al(2)]

Once the unperturbed parameters had been obtained, the next experimental task was to set up a pair-breaking boundary condition over one face of the sample, with everything else unchanged. However, because of the well-known effect of strains, two different specimens were not expected to exhibit rigorously the same superconducting characteristics, though they were cut out of the same foil and glued on the substrate under conditions which outwardly looked identical. Therefore the actual specimen used for the unperturbed state measurements was subsequently treated without being detached from the substrate. In this way the effect of the stresses resulting from the handling and mounting of the foil was the same in the two cases. On the other hand, one could not adequately get rid of the oxide layer on the surface of the slab. Consequently sample Al(1) was transformed into Al(2) by implanting on its free surface a dose of around  $10^{16}$  gadolinium ions/cm<sup>2</sup> at a total energy of 80 keV. This corresponds to a mean penetration depth of 300 Å.

Then the question arises of the influence of stresses induced by the implantation itself. The stress within the 300 Å thick implanted layer does not exceed the tensile strength of the material,

say  $10^{10}$  dyn/cm<sup>2</sup>. Since the aluminum slab is bonded to the 0.3-mm-thick sapphire substrate strongly enough to suppress slippage, the resulting stress in the bulk of the sample may be estimated to be less than  $10^6$  dyn/cm<sup>2</sup>. Such a stress is known to have negligibly small effects on the superconducting properties of aluminum.<sup>12</sup> Thus the stress in the bulk of the aluminum is expected to be unchanged for the two specimens.

On the other hand, the conditions prevailing within the implanted layer are not simple. However, if the layer gives any contribution by itself to the specific-heat difference of the whole sample, this contribution is vanishingly small considering the thickness ratio which is about  $10^{-3}$ . Then the predominant effect of the implanted layer comes from the effective pair-breaking condition which is actually achieved:  $[\Delta(x)]_{x=0}$  may be different from zero, but such a situation is still relevant to the FM theory.

A new set of data, the perturbed state data, were taken on sample Al(2). The results are repre-

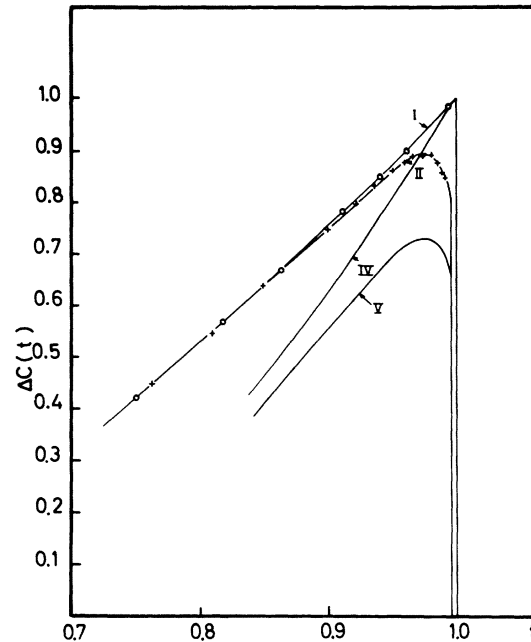


FIG. 2. Reduced differences between the specific heats of the superconducting and normal states.  $\Delta C = \Delta\bar{C}/\Delta\bar{C}_0$ , as a function of the reduced temperature  $t = T/T_{c_0}$ , with  $\Delta\bar{C}_0 = 2.21$  mJ/mole K and  $T_{c_0} = 1.183$  K. Circles (○) are experimental points from measurements on sample Al(1) (pure aluminum foil). Crosses (+) are experimental data on sample Al(2) (the same sample as before after it has been implanted with gadolinium ions). Curve IV is calculated from FM theory for an unperturbed sample and curve V is calculated for a perturbed sample with  $d_s/\Lambda(t_c) = 24$  and  $\Delta(0) = 0$ .

sented in Fig. 2 and yield the following conclusions: (a) At the lowest temperatures there is no measurable difference between the perturbed and unperturbed state values of the reduced specific-heat difference  $\Delta C(t)$ , and the FM theoretical deviation is qualitatively reproduced near the critical point. (b) The observed shift in the reduced transition temperature,  $1 - t_c = (4.2 \pm 1.7) \times 10^{-3}$ , agrees with the value of  $4.3 \times 10^{-3}$  which is calculated from theory. However, the experimental accuracy is not sufficient to provide a definitive check of theory on this point. (c) On the other hand, the experimental value of the reduced specific-heat jump  $\Delta C(t_c) = 0.81 \pm 0.02$  appears to be definitely greater than the theoretical prediction  $\Delta C(t_c) = 0.666$ .

This result suggests that the pair-breaking effect at the boundary is not strong enough to fully cancel the order parameter. Since the boundary is undoubtedly not clean, the scattering of electrons by lattice defects and by gadolinium impurities is likely to allow a steep variation of the pair potential within the implanted layer<sup>13</sup> and  $[\Delta(x)]_{x=0}$  is not strictly zero. According to the FM hypothesis, when small deviations from the boundary condition occur, we can write  $\Delta(0)/\Delta(d_s) = a$ , where  $a$  is assumed to be temperature independent near  $T_c$ . Then the critical temperature and the reduced specific-heat jump are given by<sup>14</sup>

$$\ln t_c = - [a' \Lambda(t_c) / 2d_s]^2$$

and

$$\Delta C(t_c) = \frac{3 + (4 \sin a')/a' + (\sin 2a')/2a'}{2[1 + (\sin a')/a']^2},$$

where  $a' = \pi - 2 \sin^{-1}a$ . From  $\Delta C(t_c) = 0.81$  we obtain  $a = 0.30$  and  $1 - t_c = 2.8 \times 10^{-3}$ , a value which is still compatible with the experimental one. In this respect a stronger pair-breaking effect at  $x=0$  is expected to improve the agreement between experiment and theory.

### C. Samples submitted to stray fields from an iron film

Another way of providing the boundary condition  $[\Delta(x)]_{x=0} = 0$  is to impose a magnetic field which is lower than the critical field and which is confined to a thin layer near the face  $x=0$ . This situation may be approximately achieved by the fields associated with a surface distribution of magnetic poles. A thin deposit of iron was used, in the hope that the stray fields would produce the local pair breaking. Since we wanted the magnetic field to be present only within a very thin layer of the aluminum slab, the iron to aluminum distance was varied in order to estimate the range of the fields.

Practically we operated in the following way. A

piece of aluminum foil was glued on the sample holder and then polished with diamond powder in order to obtain surface defects with typical dimensions of a few times  $10^3 \text{ \AA}$ . After a SiO film had been interposed, iron was evaporated over the slab to a thickness of about  $200 \text{ \AA}$ . Two samples were prepared by this method: Al(3) with an evaporated  $4.300\text{-\AA}$ -thick SiO film and Al(4) with a  $600\text{-\AA}$ -thick one. In either case an examination of the evaporated films under the microscope revealed no obvious difference in the defects which were formed on them. As previously discussed in the case of sample Al(2), the sample-substrate bond is strong enough to rule out the occurrence of strong mechanical stresses produced by the SiO and Fe deposits. In addition, polishing has certainly not a drastic effect on samples which, in any case, have been cold worked before. But it must be outlined that the two samples were prepared separately and, consequently, the stresses produced by handling and mounting are likely to differ in the two cases. Then the unperturbed states for samples Al(3) and Al(4) are not expected either to be identical or to be very accurately represented by sample Al(1) data.

The temperature dependence of the difference between the superconducting and normal-state specific heat  $\Delta \bar{C}(T)$  is given for samples Al(3) and Al(4)

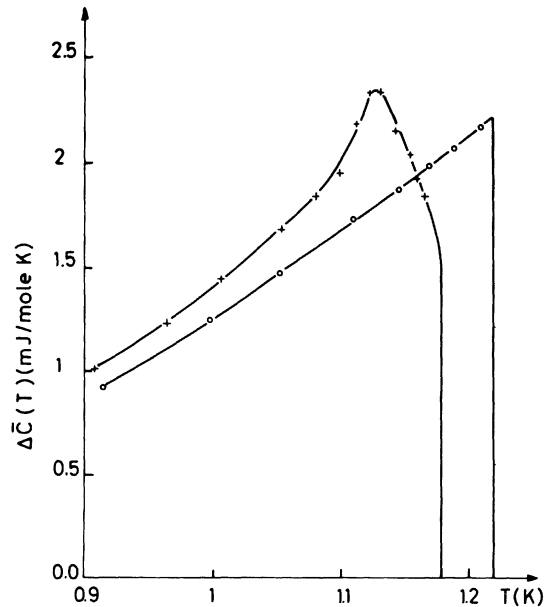


FIG. 3. Difference between the specific heats of the superconducting and normal states,  $\Delta \bar{C}(T)$ , as a function of temperature, for samples Al(3) and Al(4). Circles (○) are experimental points from measurements on sample Al(3) (aluminum foil plus  $4.300\text{-\AA}$  SiO film plus iron deposit), and crosses (+) are data on sample Al(4) (aluminum foil plus  $600\text{-\AA}$  SiO film plus iron deposit).

in Fig. 3, where reduced coordinates have not been used since  $T_{c0}$  and  $\Delta\bar{C}_0$  were not exactly known. The shape of the curve for sample Al(3) is essentially the same as that obtained with sample Al(1). Only slight differences appear from a quantitative point of view. We observe  $T_c = 1.219 \pm 0.001$  K instead of  $T_{c0} = 1.183 \pm 0.001$  K, but  $\Delta\bar{C} = \Delta\bar{C}_0$  within experimental accuracy. From these results two conclusions can be drawn. First, the magnetic fields of the iron deposit do not appreciably affect the specific-heat difference of aluminum, even in the vicinity of  $T_c$ , so the field can be estimated to have a range shorter than  $5.000 \text{ \AA}$ . Second, the stresses produced by handling and mounting of the samples are presumably responsible for the shift observed in the transition point, but, in any case, they do not affect the shape of the transition, and no measurable smearing occurs at the specific-heat jump. The curve for sample Al(4), however, exhibits a drastically different shape. It can be inferred that the stray fields are now operative, and, according to the foregoing estimation, their range is less than 2% of the aluminum thickness. The observed value of the transition point  $T_c = 1.178 \pm 0.002$  K is not more significant than before, but the specific-heat jump  $\Delta\bar{C} = 1.55 \pm 0.02$  mJ/mole K is considerably depressed. As the temperature is lowered below  $T_c$ , the specific-heat difference rises rapidly and goes through a bump with a maximum near  $T = 1.125$  K, and then smoothly recovers the typical variation of the unperturbed state. This behavior is consistent with the assumption of stray fields being confined to a thin layer near the face  $x = 0$ . At the lowest temperatures the superconducting state is not appreciably disturbed throughout the sample, but, as temperature is increased the fields gradually destroy the superconducting state within the layer in which they are present, giving rise to a smeared-out first-order transition. Then the boundary condition  $[\Delta(x)]_{x=0} = 0$  can be considered to prevail, and the experimental situation should correspond to that of the FM model right at  $T_c$ . If that is the case we can reasonably assume further that the magnitude of the specific-heat jump corresponding to the unperturbed state of sample Al(4) should be rather closely approximated by the value  $\Delta\bar{C}_0$  which has been observed in sample Al(1) and in sample Al(3) as well. Then we obtain for Al(4) a reduced specific-heat jump of 0.7, which is in fairly good agreement with the theoretical prediction.

#### IV. EXPERIMENTS ON TIN FILMS

The proximity effect gives a straightforward method of providing a pair-breaking boundary condition, but, in the case of aluminum, it was hard

to prepare specimens with the required physical characteristics and therefore more indirect methods were used. In pure tin the zero-temperature coherence length is shorter ( $\xi_0 = 0.23 \mu\text{m}$ ) so that the thicknesses of the layers of interest for the present study are in the range of a few microns. Such specimens can be conveniently obtained by vacuum deposition, without any subsequent complications concerning the adhesion between the film and the substrate. However, when dealing with the preparation of the specimens, it must be kept in mind that the superconducting properties are strongly influenced by the deposition parameters and by stress arising in the films, and that the proximity effect is very sensitive to the electron transmission at the boundary. On the other hand, when considering the specific-heat measurements it must be stressed that because the samples are much smaller and the transition temperature higher than they were in the foregoing experiments, higher resolution is required.

##### A. Sample preparation and description

The samples were prepared by vacuum deposition from a resistively heated molybdenum crucible. During the evaporation the residual pressure was less than  $10^{-6}$  Torr and the deposition rate about  $100 \text{ \AA}/\text{sec}$ . The films were deposited on single-crystal sapphire substrates at room temperature since, in the present state of the experimental arrangement, it was unavoidable to expose the specimens to atmosphere before completing the experiments. These circumstances ruled out the possibility of studying successively the unperturbed and perturbed states of tin on the same film, so different films were required to achieve the two situations. A complication then arises from the well-known fact that the transition temperatures of tin films change significantly from specimen to specimen even when all known deposition parameters are reproduced.<sup>15,16</sup> In order to minimize this effect the samples to be compared were prepared during the same evaporation run: after several tin films had been simultaneously evaporated, a magnetic film was superimposed over some of them. The superimposition was achieved within a time interval shorter than a few seconds in order that the interface would be as clean as possible.

The evaporated magnetic material was chromium. The solid solubility of chromium in tin is negligible<sup>17</sup> which is a safeguard against interdiffusion effects. In fact it would be expected that a ferromagnetic material would produce a stronger pair-breaking effect than chromium,<sup>18</sup> but the antiferromagnetic properties of the latter ensure that

TABLE I. Some data concerning the Sn and Sn-In specimens.

Specimen label	Pair-breaking boundary condition	Weight of the superconducting layer $W$ ( $10^{-3}$ g)	Thickness of the superconducting layer $d_s$ ( $\mu\text{m}$ )	$\Delta\bar{C}$ ( $\mu\text{J/g K}$ )	$T_c$ (K)	$\Delta C$	$t_c$
Sn(1)	no	0.89	1.13	97	3.863	1.02	0.999
Sn(2)	yes	1.24	1.59	77.5	3.770	0.81	0.975
Sn(3)	no	1.74	2.23	93.5	3.871	0.98	1.001
Sn(4)	yes	2.10	2.69	80	3.835	0.84	0.992
Sn-In(1)	no	1.42	1.82	92.5	3.752	1.00	1.000
Sn-In(2)	yes	1.48	1.89	60.5	3.740	0.65	0.997

the penetration of stray fields from the magnetic film into the superconductor is negligible whatever the interface roughness may be.

To minimize further the effect of irregularities at the interface on the pair-breaking condition it is valuable to shorten the electron mean free path in the superconducting material. This was achieved by additional experiments where Sn-4-wt%-In alloys were used instead of pure tin.

Finally four pure tin films were evaporated at the same time and a 300-Å-thick chromium film was superimposed over two of them. These were: samples Sn(1) and Sn(3) without chromium (unperturbed state), Sn(2) and Sn(4) with chromium (perturbed state). In another evaporating run two Sn-4-wt%-In films were prepared with a 300-Å-thick chromium film superimposed over one of them. These were: sample Sn-In(1) (unperturbed state) and Sn-In(2) (perturbed state). The weights  $W$  and the thicknesses  $d_s$  of the superconducting films in the six samples are given in Table I. The  $W$ 's were determined with an accuracy of  $2 \times 10^{-5}$  g.

In order to measure the electron mean free path  $l$  two resistivity probes were evaporated simultaneously with the specific-heat specimens. For pure tin we obtained  $l(\text{Sn}) \approx 10.000$  Å, hence:  $\Lambda(t_c) \approx 1560$  Å, a value which is very near the clean limit value 1690 Å. In the dirty limit we found a value which is in good agreement with previous results on bulk specimens<sup>19</sup>:  $l(\text{Sn-In}) \approx 560$  Å, hence  $\Lambda(t_c) \approx 810$  Å.

### B. Heat-capacity measurements

Figure 4 presents typical results obtained in the heat-capacity measurements and shows clearly that the difference between the superconducting and normal-state heat capacities,  $\Delta C^*(T) = C_s^*(T) - C_n^*(T)$ , is an order of magnitude smaller than the background contribution. However, with an amplitude of  $10^{-2}$  K for the measuring thermal oscillations, the limit of resolution in the heat-capacity measurements could be made as low as

a few  $10^{-10}$  J/K which is enough for  $\Delta C^*(T)$  to be estimated with good precision. This is clearly demonstrated by Fig. 5 where  $\Delta C^*/T$  has been plotted versus  $T$ ,  $\Delta C^*(T)$  being obtained in the following way: the normal-state data were fitted to the expression  $C_n^*(T) = aT + bT^3 + cT^5$  by a least-square routine, and then subtracted from the superconducting state data. However, it must be noted that the size of the temperature oscillations induced some rounding of the heat-capacity curve near the transition point.

In order to get a good localization of  $T_c$ , as well as a clear determination of the heat-capacity dis-

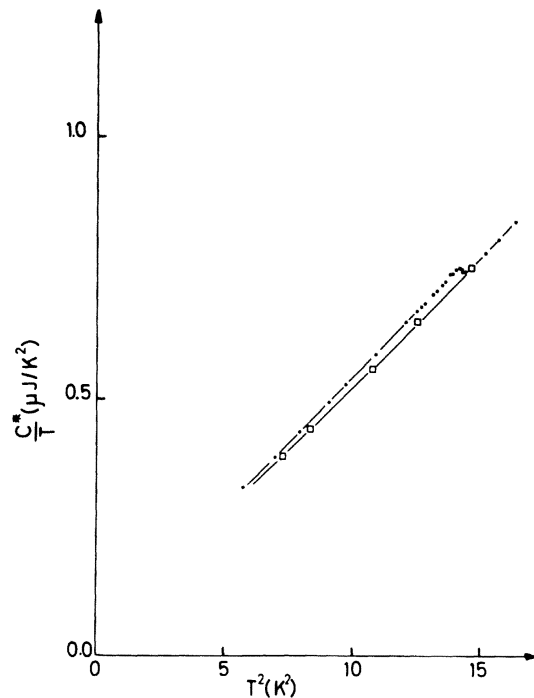


FIG. 4. Raw data for the heat capacity of sample Sn(2) with sample holder, in the superconducting state (●), and in the normal state (□). Sn(2) is a 1.59- $\mu\text{m}$ -thick pure tin film with a 300 Å thick chromium film superimposed.

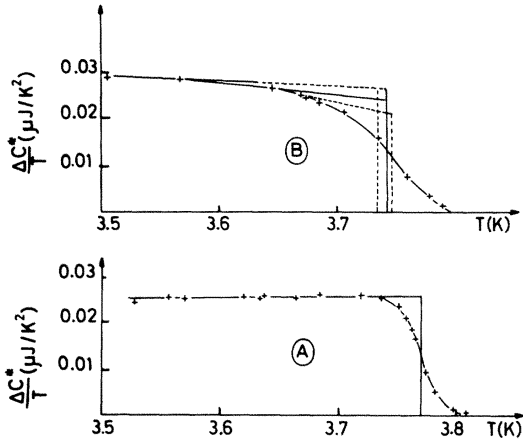


FIG. 5. Differences between the heat capacities of the superconducting and normal states for samples Sn(2) (curve A) and Sn-In(2) (curve B). Sn(2) is a 1.59- $\mu\text{m}$ -thick tin film, with a 300  $\text{\AA}$  thick chromium film superimposed. Sn-In(2) is a 1.48- $\mu\text{m}$ -thick film of Sn-4-wt. % In alloy, with a 300  $\text{\AA}$  thick chromium film superimposed. Behavior of curve A is typical of those obtained for all the Sn and Sn-In samples, with the exception of Sn-In(2). In B, the dotted lines mark the ways the experimental curve could be extrapolated in the transitional region, yielding approximate limits for  $\Delta C^*$ .

continuity at  $T_c$ , we have constructed an ideal behavior, exhibiting an infinitely steep transition and fulfilling the two requirements that, outside the critical region, both the heat capacity and entropy differences between the superconducting and normal states were identically equal to the experimentally observed values. The curve of  $\Delta C^*/T$  vs  $T$ , just as it was given by experiment below the critical region, was extrapolated to higher temperatures and assumed to fall abruptly to zero at a point which was localized so as to ensure that the areas under the ideal and the experimental curve were equal. This point was taken as the transition point, and the extrapolated value of  $\Delta C^*$  at this point was taken as the heat-capacity jump. The procedure was quite straightforward for all the samples, if one excepts sample Sn-In(2) for which the curvature of  $\Delta C^*/T$  vs  $T$  below the transition made the extrapolation a little uncertain (see Fig. 5). However, if the critical temperature in this case could be estimated independently of the heat-capacity measurements, then the above procedure would yield the heat-capacity jump with the same accuracy as before. The specific-heat data were deduced from these results. Owing to the various sources of errors, the values of the specific-heat difference  $\Delta\bar{C}$  were estimated to carry an uncertainty of 2.5% and the reduced values  $\Delta C$  an uncertainty of 5%.

## C. Critical temperature results

### 1. Pure tin

As already mentioned there is a considerable scatter in the critical temperature of pure tin films, even when they are evaporated under conditions which outwardly look identical. It has been shown that the critical temperatures depend upon the stress in the film and vary according to the orientation of the crystallites.<sup>15</sup> Since the orientation in any one film may vary from area to area, the transition is likely to be spread over an appreciable interval of temperature. Actually the effective transition widths which have been observed in rather thick films are typically of the order of  $10^{-2}$  K. From these results it may be expected that the critical temperatures of films such as ours, which were simultaneously evaporated, range within  $10^{-2}$  K. This is confirmed by our results on the pure tin films [samples Sn(1) and Sn(3)] where the critical temperatures actually differ by  $8 \times 10^{-3}$  K (see Table I). Hence the unperturbed-state transition point  $T_{c_0}$  is not known to better than  $10^{-2}$  K:  $T_{c_0} = 3.867 \pm 0.010$  K. Nevertheless, this uncertainty is definitely smaller than the shifts observed for samples Sn(2) and Sn(4) (perturbed state). The reduced critical temperatures for the series of tin samples which appear in Table I have been calculated with this value of  $T_{c_0}$  which is slightly greater than the value of 3.722 K previously reported for bulk tin.<sup>20</sup>

### 2. Sn-In alloys

Smith *et al.*<sup>19</sup> have measured the critical temperatures for a series of Sn-In alloys spanning the range of composition from 0 to 6-wt% In. For the Sn-4-wt%-In alloy the critical temperature was observed to be 0.1 K lower than in pure tin. This result is in satisfactory agreement with the present experiments where a shift of 0.115 K was observed since it must be kept in mind that our data concern films which were evaporated separately.

### 3. Comparison with FM theory

In Fig. 6 the changes in the reduced temperatures have been plotted versus  $\alpha = [\pi \Lambda(t_c)/2d_s]^2$  for all the samples which are representative of the perturbed state of the superconductor, that is samples Al(2), Sn(2), Sn(4), and Sn-In(2). For comparison FM predictions have been plotted too, first in the case of an extremely strong pair-breaking effect at the boundary, i.e.,  $\Delta(0) = 0$ , and second, in the case of a weaker effect, i.e.,  $\Delta(0) = a\Delta(d_s)$  with  $a = 0.30$ . For small values of the critical temperature shifts [samples Al(2) and Sn-In(2)] it cannot be decided whether the boundary



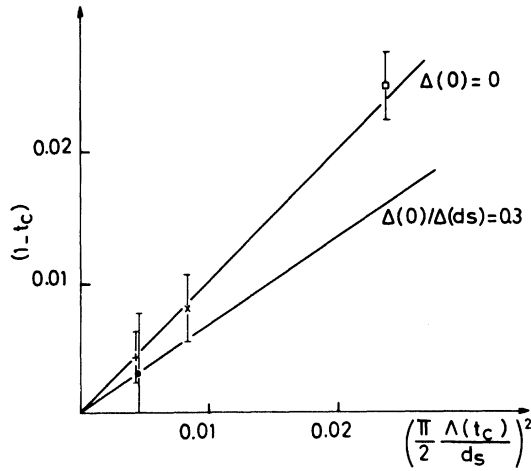


FIG. 6. Shifts in the critical temperature  $(1-t_c)$  as a function of  $\alpha = [\pi\Lambda(t_c)/2d_s]^2$  for sample Al(2) (+), Sn(2) ( $\square$ ), Sn(4) ( $\times$ ), Sn-In(2) ( $\bullet$ ). Solid lines are calculated from FM theory with  $\Delta(0)=0$  and  $\Delta(0)/\Delta(d_s)=0.3$ , respectively.

condition  $\Delta(0)=0$  actually holds or not, but the results on samples Sn(2) and Sn(4) are more conclusive in this respect. This situation results partly from the experimental difficulty in obtaining reproducible results on the transition temperature of evaporated films, but, above all, it illustrates the fact already emphasized by FM that the change in transition temperature is not a sensitive measure of the proximity effect especially in the case of rather thick films.

#### D. Specific-heat jump results

##### 1. Unperturbed samples

The unperturbed samples of pure tin [samples Sn(1) and Sn(3)] yield two values for the specific-heat jump in the unperturbed state which are consistent with one another within the experimental accuracy, so that  $\Delta\bar{C}_0 = 95 \pm 2.5 \mu\text{J/g K}$ . This value is larger than that obtained with bulk tin samples:  $88.9 \mu\text{J/g K}$ .<sup>20</sup> This is to be compared with the enhancement in the transition point which has been pointed out before. Such a behavior may be attributed to thin-film effects.

For the dirty specimen Sn-In(1), on the other hand, the specific-heat jump  $\Delta\bar{C}_0 = 92.5 \pm 2.5 \mu\text{J/g K}$ , and the transition point are reduced by a few percent as compared to the values of the pure tin films. This is exactly what one would have expected for impure tin samples.

These values of  $\Delta\bar{C}_0$ , and those for  $T_{c0}$  quoted before, have been used to calculate the reduced quantities  $\Delta C$  and  $t$  which are plotted in Fig. 7 and 8 for pure tin specimens and dirty specimens, re-

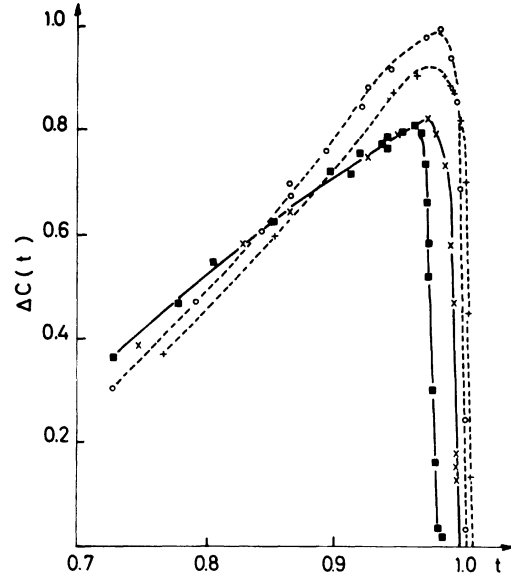


FIG. 7. Reduced differences between the specific heats of the superconducting and normal states as a function of temperature for the series of pure tin samples: Sn(1) ( $\circ$ ), Sn(2) ( $\blacksquare$ ), Sn(3) (+), and Sn(4) ( $\times$ ).  $\Delta C = \Delta\bar{C}/\Delta\bar{C}_0$ ,  $t = T/T_{c0}$ ,  $\Delta\bar{C}_0 = 95 \mu\text{J/g K}$  and  $T_{c0} = 3.867 \text{ K}$ . Dotted lines were chosen as the best representation of the data for the unperturbed samples [Sn(1) and Sn(3)] and the solid lines for the perturbed samples [Sn(2) and Sn(4)].

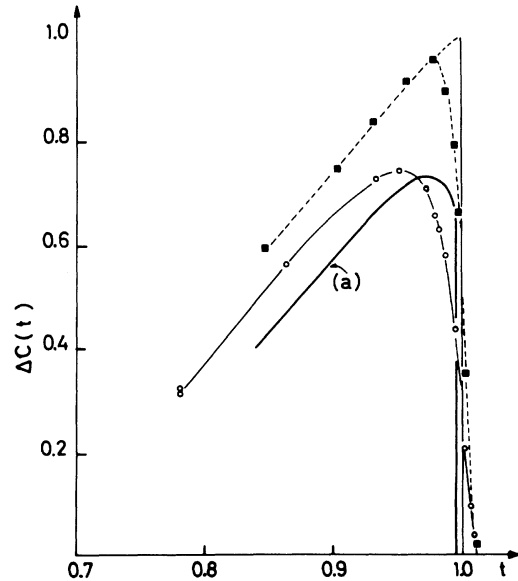


FIG. 8. Reduced differences between the specific heats of the superconducting and normal states as a function of temperature for the Sn-4-wt. %In alloys: unperturbed sample Sn-In(1) ( $\blacksquare$ ), perturbed sample Sn-In(2) ( $\circ$ ). Curve (a) is calculated from FM theory for a perturbed sample with  $d_s/\Lambda(t_c) = 34$  and  $\Delta(0) = 0$ .

spectively. It may be noted that the observed slope in the reduced specific-heat differences for the unperturbed samples near their critical points is  $(d\Delta C/dt)_{t=t_c} = 2.5 \pm 0.3$  in good agreement with the previous results on pure aluminum and the theoretical value of 2.63 which is predicted by an accurate Landau-Ginzburg theory.<sup>2</sup>

## 2. Perturbed samples

It is clear from the curves in Figs. 6 and 7, and the data in Table I, that the specific-heat jumps are markedly depressed in the samples which are perturbed by proximity effect. However, in samples Sn(2) and Sn(4) the theoretical reduction factor of 0.66 is not actually obtained. Following FM we may tentatively assume that the boundary condition takes the form  $\Delta(0) = a\Delta(d_s)$  where  $a$  is a constant independent of  $t$  and of the order of 0.3. So doing the experimental data on the specific-heat jump are brought into satisfactory agreement with the theoretical prediction, but then a discrepancy, which is larger than the experimental uncertainty, appears between the experimental and theoretical values of the shifts in the transition points: this is particularly clear in the case of sample Sn(2) (see Fig. 6). However, such an approach is certainly incorrect in the clean limit; instead the ratio  $\Delta(0)/\Delta(d_s)$  is expected to increase with  $t_c - t$ , yielding a specific heat greater than the theoretical prediction just below  $t_c$ .

In the case of the dirty specimen Sn-In(2), the curvature of the experimental curve mentioned earlier means that the specific-heat jump can be quite accurately determined only if the transition point is known independently. But the reduction factor in the specific-heat jump is obviously greater than in the clean case. If the critical temperature is assumed to be just what is predicted by theory, that is  $t_c = 0.9955$ , then the specific-heat jump is found to be  $\Delta C = 0.65$ , when the same procedure as before is followed in analyzing the data. The experimental curve of  $\Delta C$  vs  $t$  is compared to the theoretical one in Fig. 8: the same behavior is actually observed, in spite of the differences owing to the inadequacy of theory below  $T_c$  and to the broadening of the experimental transition. Thus it is concluded that the boundary condition  $\Delta(0) = 0$  holds in sample Sn-In(2).

The difference observed between the clean situation and the dirty one is easily understood. It is

very well known<sup>21</sup> that, in the clean limit, the actual value of the pair potential at the boundary is very sensitive to the electron transmission properties of the interface, whereas, in the dirty limit, electron diffusion processes at the impurities considerably decrease the relative importance of the interface defects.

## V. CONCLUSIONS

As a check of FM theory on the thermodynamical properties of superconductors with pair-breaking boundary conditions, the heat capacities of various superconducting slabs and films have been measured. The physical conditions in these systems were much better defined than those in lamellar eutectic alloys, allowing a quantitative comparison between experiment and theory. The following conclusions could be drawn: FM theory correctly predicts the specific-heat jumps, right at the transition and the shifts in the critical temperatures, but it fails to adequately describe the behavior of the specific-heat difference in any finite interval of temperature below  $T_c$ . Furthermore when deviations from the boundary condition  $\Delta(0) = 0$  occur, the assumption  $\Delta(0)/\Delta(d_s) = \text{const}$  does not seem quite realistic. The present experiments suggest rather that  $\Delta(0)/\Delta(d_s)$  is temperature dependent.

Nevertheless, the main theoretical predictions are experimentally verified. The observed specific-heat jumps are in quantitative agreement with theory whenever the pair-breaking effect is made insensitive to the defects at the boundary. Such a situation prevails in samples Al(3) and Sn-In(2). On the other hand, the shifts in the critical temperatures appear to be consistent with theory whenever the transition is sharp enough to be accurately localized, which is the case of samples Sn(2) and Sn(4). Unfortunately it is rather hard to set up a situation which meets both requirements simultaneously, since, by shortening the electron mean free path in the superconducting material, the spurious effects of the interface defects are minimized but an appreciable smearing of the transition appears.

## ACKNOWLEDGMENTS

The authors are grateful to Professor E. Guyon for helpful discussions and to Dr. J. Chaumont for the ionic implantations.

\*Laboratoire associé au CNRS.

<sup>1</sup>P. Fulde and W. Moormann, Phys. Kondens. Mater. **6**, 403 (1967).

<sup>2</sup>L. Gunther, G. Deutscher, and Y. Imry, Phys. Rev.

B **7**, 3393 (1973).

<sup>3</sup>C. A. Schiffman, J. F. Cocheran, and M. Garber, Rev. Mod. Phys. **36**, 127 (1964); J. Lechevet, J. E. Neighbor, and C. A. Schiffman, Phys. Rev. B **5**, 861 (1972).

- <sup>4</sup>P. Manuel and J. J. Veyssié, *Phys. Lett. A* 41, 235 (1972); *Solid State Commun.* 13, 1819 (1973).
- <sup>5</sup>P. F. Sullivan and G. Seidel, *Phys. Rev.* 173, 679 (1968).
- <sup>6</sup>P. Manuel, H. Niedoba, and J. J. Veyssié, *Rev. Phys. Appl.* 7, 107 (1972).
- <sup>7</sup>P. Manuel, H. Niedoba, and J. J. Veyssié, *Bull. Inf. Bur. Nat. Métrol. (France)* 14, 9 (1973).
- <sup>8</sup>The germanium thermometer has been calibrated above 1.5 K by the Service des Basses Températures C.E.N.G. (Grenoble).
- <sup>9</sup>P. Manuel and J. J. Veyssié, *Rev. Gen. Therm.* 136, 337 (1973).
- <sup>10</sup>P. Manuel, thesis (Université Paris XI-Orsay, (1974) (unpublished); P. Manuel and J. J. Veyssié, *Rev. Gen. Therm.* (to be published).
- <sup>11</sup>D. C. Rorer, H. Meyer, and R. C. Richardson, *Z. Naturforsch. A* 18, 130 (1963).
- <sup>12</sup>H. A. Notarys, *Appl. Phys. Lett.* 4, 79 (1964).
- <sup>13</sup>J. J. Hauser, H. C. Theuerer, and N. R. Werthamer, *Phys. Rev.* 142, 118 (1966).
- <sup>14</sup>K. Maki, in *Superconductivity*, edited by R. D. Parks (Marcel Dekker, New York, 1969), Chap. 18.
- <sup>15</sup>R. H. Blumberg and D. P. Seraphim, *J. Appl. Phys.* 33, 163 (1962).
- <sup>16</sup>R. E. Miller and G. D. Cody, *Phys. Rev.* 173, 494 (1968).
- <sup>17</sup>F. A. Shunk, *Constitution of Binary Alloys*, 2nd ed. (McGraw-Hill, New York, 1969).
- <sup>18</sup>P. G. de Gennes and G. Sarma, *J. Appl. Phys.* 34, 1380 (1963).
- <sup>19</sup>F. W. Smith, A. Baratoff, and M. Cardona, *Phys. Kon-dens. Mater.* 12, 145 (1970).
- <sup>20</sup>J. F. Cocheran, *Ann. Phys. (N.Y.)* 19, 186 (1962).
- <sup>21</sup>P. G. de Gennes, *Rev. Mod. Phys.* 36, 225 (1964).